Research Article 研究报告

利用副干酪乳酪杆菌 SCFF20 高效生物合成纳米硒颗粒：一种潜在的亚硒酸盐生物转化工厂

赵志峰 [1,2#]，曹雨澜 [1#]，陈晓蝶 [1]，王佐军 [2]，徐腾 [1]，熊大可 [1]，胡陆军 [1*]

1 四川轻化工大学生物工程学院 四川省白酒酿造生物技术及应用重点实验室，四川 宜宾 644005
2 四川大学生物质科学与工程学院，四川 成都 610000

摘　要：【目的】硒(Se)是人体必需的微量元素，在维持人体生理代谢中起着至关重要的作用。在硒的各种形态中，纳米硒颗粒(selenium nanoparticles, SeNPs)被发现具有较高的生物利用度和较低的毒性。本研究拟筛选一株能将亚硒酸盐高效合成纳米硒颗粒的益生菌菌株。【方法】从 14 株潜在益生菌中筛选出一株能有效将亚硒酸钠转化为 SeNPs 的耐硒菌株副干酪乳酪杆菌 SCFF20。利用扫描电子显微镜 X 射线能量色散谱仪(scanning electron microscopy coupled with energy-dispersive X-ray, SEM-EDX)、动态光散射(dynamic light scattering, DLS)、X 射线衍射仪(X-ray diffractometer, XRD)、拉曼光谱(Raman spectroscopy)和傅里叶变换红外光谱(Fourier transform infrared spectroscopy, FTIR)对副干酪乳酪杆菌 SCFF20 产生的 SeNPs 进行纯化、冷冻干燥和系统表征。【结果】SEM-EDX 分析表明，Se 是生物纳米硒颗粒的主要成分。合成的 SeNPs 呈球形、多分散、平均粒径约为 500.62 nm。XRD 图谱和拉曼光谱证实所制备纳米硒颗粒的生物无定形性质。FTIR 分析证明蛋白质、胞外多糖和脂质包覆在 SeNPs 表面。电感耦合等离子体发射光谱(inductively coupled plasma-optical emission spectroscopy, ICP-OES)测得 SeNPs 的还原率为 91.42%。【结论】本研究证实了副干酪乳酪杆菌 SCFF20 作为纳米硒生产益生菌的潜力，可作为

安全生产生物源纳米硒的生物工厂以便用于营养补充剂和功能食品。

关键词：细菌还原作用；益生菌；副干酪乳酪杆菌；纳米硒颗粒

Efficient biosynthesis of selenium nanoparticles by *Lacticaseibacillus paracasei* SCFF20: a potential cell factory for selenite conversion

ZHAO Zhifeng[1,2#], CAO Yulan[1#], CHEN Xiaodie[1], WANG Zuojun[2], XU Teng[1], XIONG Dake[1], HU Lujun[1*]

1 Liquor Making Biotechnology and Application Key Laboratory of Sichuan Province, College of Biological Engineering, Sichuan University of Science and Engineering, Yibin 644005, Sichuan, China
2 College of Biomass Science and Engineering, Sichuan University, Chengdu 610000, Sichuan, China

Abstract: [Objective] Selenium (Se) is an essential trace element playing a critical role in maintaining the physiological metabolism of humans. Among its various forms, selenium nanoparticles (SeNPs) possess higher bioavailability and lower toxicity. The study aims to screen a probiotic strain that can efficiently synthesize SeNPs from selenite. **[Methods]** *Lacticaseibacillus paracasei* SCFF20 capable of converting sodium selenite to SeNPs was screened out from 14 strains of probiotics. The SeNPs produced by *L. paracasei* SCFF20 were purified, freeze-dried, and systematically characterized by scanning electron microscopy coupled with energy-dispersive X-ray (SEM-EDX), dynamic light scattering (DLS), X-ray diffractometer (XRD), Raman spectroscopy, and Fourier transform infrared spectroscopy (FTIR). **[Results]** SEM-EDX results revealed that Se was the primary constituent of SeNPs. The synthesized SeNPs were spherical and polydisperse, with an average particle size of 500.62 nm. XRD and Raman spectroscopy confirmed that the SeNPs were amorphous. Additionally, FTIR demonstrated the presence of proteins, exopolysaccharides, and lipids coating the surface of the SeNPs. Moreover, the reduction rate of SeNPs was determined to be 91.42% by inductively coupled plasma-optical emission spectroscopy (ICP-OES). **[Conclusion]** The findings of this study highlight the potential of *L. paracasei* SCFF20 as a probiotic strain capable of producing SeNPs. The strain can be used as a cell factory for the safe production of biogenic SeNPs as nutritional supplements and functional food.

Keywords: bacterial reduction; probiotic; *Lacticaseibacillus paracasei*; selenium nanoparticles (SeNPs)

Selenium (Se), an essential trace element, exerts significant effects on antioxidant defense, immune regulatory function, antitumor activity, and redox homeostasis in human health[1-2]. The beneficial effects of Se on human health can be attributed to its presence in many selenoproteins such as iodothyronine deiodinases, glutathione peroxidase, selenoprotein W, selenoprotein P, and thioredoxin reductase[3]. Selenium deficiency has been associated with neurodegeneration, cancer, immune dysfunction, cardiovascular diseases, hypothyroidism, and male sterility[4-5]. It affects an

approximately one billion people worldwide[6]. Diet plays a crucial role in the elemental Se intake, which depends on its concentration and speciation[7]. However, Se has a very narrow margin of safety between beneficial and toxic effects, which is closely related to its speciation[8]. Both the toxicity and bioavailability of Se are primarily determined by its speciation[9]. The recommended selenium intake for humans is 55 μg/d, and a level of about 40 μg/d is suggested as the minimum requirement to avoid deficiency. However, the tolerable upper limit for Se intake is 400 μg/d[10-11].

In nature, Se exists in various redox states, including selenate (SeO_4^{2-}, VI), selenite (SeO_3^{2-}, IV), elemental selenium (Se^0), and selenide (Se^{2-})[12]. Selenite (IV) and selenate (VI) are highly water-soluble and toxic to the human body. Additionally, research studies have indicated that selenite (IV) is the most toxic among all valence states, affecting cell respiration, enzyme activity, the cell antioxidant system, and DNA repair[13]. On the other hand, the reduction of soluble Se(IV) and Se(VI) oxyanions to insoluble Se(0) potentially serves as a detoxification strategy, due to its biocompatible and low or no cytotoxicity[14]. Selenium nanoparticles (SeNPs), representing a new form of Se(0), have emerged as a promising candidate because of their low toxicity and enhanced biological activities. Husen and Siddiqi demonstrated that SeNPs exhibited good biocompatibility and can serve as supplements to for individuals with Se deficiency[15]. Consequently, SeNPs are considered a novel and promising nutritional additive for humans.

The conventional methods used to produce SeNPs involve high temperatures and pressures. In recent years, the biosynthesis of SeNPs using microorganisms, particularly probiotics, has become a realistic approach[16]. The biosynthesis of SeNPs by probiotics is considered as a green manufacturing process due to eco-friendly, safe, and cost-effective nature[17-18]. Probiotics, which are generally recognized as safe microorganisms commonly used in food processing, have attracted attention for synthesizing SeNPs[19-20].

Moreover, the SeNPs synthesized by probiotics do not require extensive purification since the probiotics and culture medium used can be suitable as food supplements in human diets[21]. Furthermore, many probiotics can survive the gastrointestinal tract and thus serve as means to deliver beneficial and biologically active molecules such as SeNPs, to the human body[22]. Probiotics are commonly employed as starter cultures for food fermentations due to their fermenting ability, which contribute to food safety, sensorial characteristics, and health benefits[23].

In the present study, *Lacticaseibacillus paracasei* SCFF20, which exhibits high Se tolerance and biotransformation capacity, was selected from 14 well-known potential probiotics through primary screening, Se-tolerance domestication, and optimization of fermentation conditions. The biogenic SeNPs synthesized by *L. paracasei* SCFF20 were characterized using scanning electron microscopy coupled with energy-dispersive X-ray (SEM-EDX), dynamic light scattering (DLS), X-ray diffractometer (XRD), Raman spectroscopy, and Fourier transform infrared spectroscopy (FTIR). Additionally, Se(0) concentrations were determined using inductively coupled plasma optical emission spectroscopy (ICP-OES).

1 Materials and Methods

1.1 Bacterial strains

Fourteen potential probiotic strains containing *Lactiplantibacillus plantarum* (SCFF13, SCFF109, SCFF134, SCFF180, SCFF193, SCFF195), *Pediococcus pentosaceus* (SCFF18, SCFF125), *Lacticaseibacillus paracasei* (SCFF15, SCFF20), *Levilactobacillus brevis* (SCFF104), *Lentilactobacillus buchneri* (SCFF127), *Limosilactobacillus fermentum* (SCFF220), and *Lactococcus lactis* (SCFF240) in this study were obtained from the Culture Collection of Food Microorganisms of Sichuan University of Science and Engineering (Yibin, China). Cultivation of these bacteria was carried out using a de Man, Rogosa and Sharpe (MRS) medium at a temperature of 37 °C.

1.2 Se-tolerance and Se-reduction enhancement of strains

To obtain strains with high selenium tolerance and reduction capabilities, 14 strains underwent a domestication process in which they cultured in an MRS medium supplemented with increasing concentrations of Na_2SeO_3, following a previously established protocol[24]. A series of MRS culture media containing Na_2SeO_3 at concentrations ranging from 0 to 120 μg/mL, with an increment of 20 μg/mL, were prepared. The mixture cultures were incubated at 37 ℃ for 48 h. The strains were sequentially inoculated into these cultures starting from the lowest concentration of Na_2SeO_3 and processing to higher concentrations, with each concentration cultured for two generations. Selection criteria were viable bacterial and ability of the cells to convert sodium selenite to elemental Se[25-26]. The Se-tolerance capacity of these strains was assessed by determining viable bacterial counts using a protocol based on a previously published method[27], while the reducing power of the strains on Na_2SeO_3 was measured by a color change using a colorimeter (UltraScan VIS, HunterLab) to determine the shade of red in the culture.

1.3 Single-factor optimization experiments

The conditions for Se-enrichment were optimized, taking into account temperature, shaking speed, Se(IV) exposure time, inoculation volume, and Se(IV) concentration. The determination of the amount of Se(0) was conducted according to the methodology outlined in a previous study by Biswas et al.[28]. A black powdered Se metal (Shanghai Maclin Biochemical Technology Co., Ltd.) was employed as a standard for elemental selenium. Following incubation, the bacterial culture, along with the Se(0), was collected through centrifugation at 8 000 r/min for 10 min. The resulting pellets were then subjected to two washes with a sodium chloride solution (1 mol/L). The red colloidal selenium present in the pellet was dissolved in 15 mL Na_2S (1 mol/L). Subsequently, bacterial cells were removed by centrifugation, and the absorbance of the resulting red-brown solution was measured at a wavelength of 500 nm using a spectrophotometer.

1.3.1 Preparation of inoculum of *L. paracasei* SCFF20

A 500 μL aliquot of *L. paracasei* SCFF20 culture was streaked onto a MRS agar plate and incubated at 37 ℃ for 24 h to allow growth. A single colony was then inoculated into a tube and incubated at 37 ℃ for 24 h in a shaking incubator at a speed of 120 r/min, and the optical density at 600 nm (OD_{600}) of *L. paracasei* SCFF20 culture was approximately 5.73. Subsequently, a 2 mL volume of the inoculum was transferred to a 100 mL of MRS culture medium allowed to continue growing for another 24 h at 37 ℃ at a shaking speed of 120 r/min, resulting in the culture undergoing two generations of growth.

1.3.2 Effect of temperature on the selenate reduction

To examine the impact of temperature, a 100 mL MRS culture medium with 100 μg/mL Na_2SeO_3 was prepared in a shaking tube. A 2 mL inoculum was added to the medium, and the tube was incubated at temperatures of 28, 31, 34, 37, 40, and 43 ℃ with a shaking speed of 120 r/min for a duration of 24 h. The amount of Se(0) was determined by measuring the optical density at 500 nm (OD_{500}) of the bacterial cultures, employing the previously mentioned methodology.

1.3.3 Effect of shaking speed on the selenate reduction

To investigate the impact of shaking, a 2 mL of inoculum was added to 100 mL of MRS culture medium supplemented with 100 μg/mL Na_2SeO_3. Each experimental set was incubated at a temperature of 37 ℃ for a duration of 24 h, employing different shaking speeds of 90, 120, 150, 180, 210, and 240 r/min. The amount of Se(0) was determined by measuring the optical density at 500 nm (OD_{500}) of the bacterial cultures, utilizing the previously described methodology.

1.3.4 Effect of Se(IV) exposure time on the selenate reduction

For investigating the influence of Se(IV) exposure time on the growth *L. paracasei* SCFF20, a shaking tube containing 100 mL of MRS

medium supplemented with 100 μg/mL Na_2SeO_3 was prepared. A 2 mL volume of inoculum was added to the medium and subjected to incubation at a shaking speed of 180 r/min. The incubation period varied and included durations of 8, 12, 16, 20, 24, 28, 32, 36, 40, 44, 48, and 52 h. The amount of Se(0) was quantified by measuring the optical density at 500 nm (OD_{500}) of the bacterial cultures using the aforementioned methodology.

1.3.5 Effect of inoculum volume on the selenate reduction

For investigate the impact of inoculum volume on the system, different of inoculum, including 0.5, 1, 2, 3, 4 and 5 mL, were separately added to volumes of MRS medium supplemented with 100 μg/mL Na_2SeO_3, namely 99.5, 99, 98, 97, 96, and 95 mL, respectively. Each experimental set was incubated for a duration of 24 h at a temperature of 37 °C, employing a shaking speed of 180 r/min. The amount of Se(0) was determined by measuring the optical density at 500 nm (OD_{500}) of the bacterial cultures using the above-mentioned methodology.

1.3.6 Effect of the selenium concentration on the selenate reduction

To perform the Se tolerance test, a 2 mL bacterial culture was aseptically added to 100 mL of MRS liquid medium supplemented not added yet Na_2SeO_3. Subsequently, sterilized Na_2SeO_3 solution was introduced to achieve final concentrations of 40, 60, 80, 100, 120 and 140 μg/mL in the system. The amount of Se(0) was determined by measuring the optical density at 500 nm (OD_{500}) of the bacterial cultures, employing the previously described methodology.

1.4 Synthesis of biogenic SeNPs

SeNPs were synthesized by *L. paracasei* SCFF20 under the aforementioned optimized Se-enrichment conditions. The synthesis procedure performed by *L. paracasei* SCFF20 was based on the established protocol outlined by Sonkusre[29] with certain modifications. Se-enriched *L. paracasei* SCFF20 cells were collected *via* centrifugation at a speed of 12 000×*g* for 20 min. The resulting pellet was washed with phosphate

buffer solution (PBS, pH 7.0) and subsequently resuspended in 20 mL of sterile water. A lysozyme solution (100 mg/mL) at a volume of 120 μL was added, and the culture was kept at a temperature of 37 °C for a duration of 3 h. The culture was then subjected to ultrasonic treatment on ice for 25 min, employing a power setting of 300 W with intervals of 5 s/5 s. The resultant slurry, comprising both SeNPs and cell fraction, was subjected to three washes with Tris-HCl solution (1.5 mol/L) containing 1% sodium dodecyl sulfate (SDS). Following this, centrifugation at 14 000×*g* for 10 min was conducted. The resulting pellet, containing both SeNPs and cell debris, was washed and resuspended in sterile water. After the addition of 1-octanol, the solution was mixed thoroughly mixed, then centrifuged at 2 000×*g* for 5 min at a temperature of 4 °C, and left undisturbed for 24 h. The upper phase and interface, which contained insoluble cell debris, were discarded, while the bottom water phase was successively washed with chloroform, absolute ethanol, 70% ethanol, and sterile water. Centrifugation at 15 000×*g* for 10 min was performed after each washing step. The resulting precipitation was washed with sterile water and subjected to freeze-drying using a lyophilizer. This sample was then used for subsequent characterization and Se(0) content.

1.5 Characterization of the biogenic SeNPs

The biogenic SeNPs synthesized by *L. paracasei* SCFF20 were subjected to characterization using various techniques, including scanning electron microscopy coupled with energy-dispersive X-ray (SEM-EDX), dynamic light scattering (DLS), X-ray diffractometer (XRD), Raman spectroscopy, Fourier transform infrared spectroscopy (FTIR), and inductively coupled plasma-optical emission spectroscopy (ICP-OES). The characterization procedures followed the protocols described in previous studies[19,30].

1.5.1 SEM-EDX

The morphological characteristics and elemental composition of the SeNPs were

investigated using scanning electron microscopy coupled with energy-dispersive X-ray (SEM-EDX). Following the growth of *L. paracasei* SCFF20, the cells were harvested by centrifugation at a speed of 6 000 r/min for 10 min at a temperature of 4 °C. Subsequently, the cells were fixed with 2.5% glutaraldehyde at 4 °C for a duration of 24 h. After undergoing three washes with 0.1 mol/L phosphate-buffered saline (PBS), the cells underwent a gradual dehydration process using a series of increasing concentrations of alcohol (30%, 50%, 70%, 80%, 90%, and 100%). The dehydrated samples were then freeze-dried, sputter coated on the copper sheet at room temperature, and subjected to SEM analysis (Tesan) at an accelerating voltage of 200 kV. Concurrently, the EDX analysis (Bruker) was conducted to analyze the extracted SeNPs.

1.5.2 DLS

The size distribution of the SeNPs was determined using dynamic light scattering (DLS) analysis performed with a Zetasizer Nano ZS90 instrument (Malvern). The SeNPs were dispersed in anhydrous ethanol and subjected to sonication for a duration of 20 min to ensure proper dispersion. An aliquot of the sample was then transferred into a quartz cuvette for measurement, and the data was recorded at a temperature of 25 °C.

1.5.3 XRD

The synthesized SeNPs were analyzed for their crystalline structure using an X-ray diffractometer (AXS). The specimens were carefully positioned on the X-ray diffractometer plate using the press-and-pull technique. The diffractogram was then obtained utilizing the Breg Brentano method with Cu Kα radiation. The scanning conditions for the samples were as follows: a 2θ range of 5°–90°, with a step size of 0.03° and an exposition time of 2 s per step.

1.5.4 Raman spectroscopy

The Raman spectroscopy analysis of the synthesized SeNPs was performed using a LabRam HR Raman spectrometer (Thermo) with 514 nm excitation (30 mW) and a spectral range of 0–3 500 cm^{-1}. To obtain the spectra, an aqueous suspension of the synthesized SeNPs was prepared and transformed into a thin film on a small piece of aluminum foil, which was subsequently air-dried at room temperature. The Raman spectra were recorded to determine the characteristics of the synthesized SeNPs. Each spectrum was collected with a 20 s interval, and the results were averaged of 10 independent runs.

1.5.5 FTIR

The characterization of functional groups present in the synthesized SeNPs' biological macromolecules was conducted using Fourier transform infrared spectroscopy (FTIR) with a Nicolet 6700 FTIR instrument (ThermoFisher Scientific Inc., Waltham). The analysis was performed using the potassium bromide (KBr) pellet technique, which enabled spectroscopy in the frequency range of 4 000−400 cm^{-1}.

1.6 Se nanoparticles content analysis

The determination of Se(0) concentrations in the synthesized nano-selenium powder was performed according to the established protocol in a previous study[31]. The nano-selenium powder obtained was subjected to acid digestion in a crucible reaction vessel, utilizing closed vessels containing 2 mL of concentrated HNO_3 and 1 mL of 30% (*V/V*) H_2O_2. After cooling, the resulting solutions were diluted to a final volume of 100 mL with Milli-Q water, and Se(0) concentrations were quantitatively analyzed using inductively coupled plasma-optical emission spectroscopy (ICP-OES) with a PerkinElmer Optima 8000 instrument. A control group of bacteria that were not exposed to Na_2SeO_3 was included for comparison. A blank consisting of the reaction mixture without the cell pellets was also prepared and accounted for in the final results. The Se reduction rate was calculated using the following formulas:

Se reduction rate=(elemental Se content in SeNPs/elemental Se content in Na_2SeO_3)×100%.

1.7 Statistical analysis

Each experiment procedure was conducted in a minimum of three independent replicates, and the obtained data were subjected to statistical

analysis using either one-way analysis of variance (ANOVA) or Student's *t*-test, depending on the experimental design, with the aid of SPSS version 19.0 software Statistical significance was determined at a significance of $P \leq 0.05$. The results were presented as means ± standard deviation (SD).

2　Results and Discussion

2.1　Analysis of Se-tolerance and Se-reduction enhancement

The Se-tolerance and Se-reduction capability of the selected 14 strains were assessed by cultivating them in an MRS liquid medium supplemented with increasing concentrations of Na_2SeO_3, ranging from 0 to 120 µg/mL (0, 20, 40, 60, 80, 100, and 120 µg/mL). The Se-tolerance of the strains was evaluated by monitoring their viability after acclimation. As demonstrated in Table 1, the viable count of most strains exhibited a substantial decrease with increasing Na_2SeO_3 concentration, particularly at higher concentrations, suggesting that Se exerted a growth-inhibitory effect on these stains. The growth inhibition observed among the strains at different concentrations of Na_2SeO_3 could be attributed to the unique species and the antioxidant system of the strains, as indicated by previous studies[32]. The possible reason was that the increased concentrations of Na_2SeO_3 can lead to greater toxicity and inhibit the growth of organisms through the production of reactive oxygen species, lipid peroxidation and decreased sulfur metabolism[24].

However, it was observed that these strains were not completely inhibited even at higher concentrations of Na_2SeO_3, indicating their strong tolerance to Na_2SeO_3. Similar findings have been reported for *Lactobacillus paralimentarius*[19] and *Lactobacillus* sp.[22]. Among the viable bacterial counts of the 14 strains, *L. paracasei* SCFF20 exhibited higher viable bacterial counts (3.8×10^8 CFU/mL) at the concentration of 100 µg/mL Na_2SeO_3, and even at the concentration of 120 µg/mL Na_2SeO_3, suggesting that its elevated Se-tolerance.

Moreover, the Se-reduction capability of these strains was evaluated by analyzing color characteristics quantified in terms of values (Table 2), where values run from negative (green) to positive (red)[33-34]. The red/green values (a*) were found to increase with increasing Na_2SeO_3 concentration, indicating a shift towards a deeper red color resulting from the reduction of Na_2SeO_3 to SeNPs[35]. Studies have shown that when levels of Na_2SeO_3 in the environment reach a certain threshold, toxic Na_2SeO_3 is reduced to produce non-toxic SeNPs, which forms part of their detoxification mechanism[36]. Ullah et al. found that *Bacillus subtilis* BSN313 reduced the soluble, toxic, colorless selenium ions to the insoluble, non-toxic, red elemental SeNPs[18]. In the study of *Bacillus megaterium*[37], *Lactobacillus reuteri*[26] and *Duganella* sp.[38], it was proved that the amount of Se(0) was accumulating with the formation of red colonies.

As shown in Table 2, each strain exhibited the highest value at specific Na_2SeO_3 concentrations. Figure 1. visually illustrates the color of the 14 strains at their highest values. Among these strains, the culture of *L. paracasei* SCFF20 showed the deepest red color and had the highest value at a concentration of 100 µg/mL Na_2SeO_3, suggesting its stronger ability to reduce Na_2SeO_3 into SeNPs. Based on aforementioned analysis of Se-tolerance and Se-reduction capabilities, *L. paracasei* SCFF20 was selected for further single-factor optimization to maximize the biotransformation of selenium.

2.2　Analysis of single factor optimization experiment results

The establishment of the Se(0) standard curve was based on the correlation between the quantity of black powdered selenium and absorption (Figure S1, the data has been submitted to the National Microbial Science Data Center, number: NMDCX0000262). The selenate reduction by *L. paracasei* SCFF20 is depicted in Figure 2. The optimal temperature for the selenate reduction by *L. paracasei* SCFF20 was determined to be 37 ℃,

Table 1 The viable bacterial counts, expressed as $\log_{10}$ (CFU/mL), of 14 stains following incubation in an MRS medium supplemented with different concentrations of Na₂SeO₃

Na₂SeO₃ (μg/mL)	Viable bacterial counts ($\log_{10}$ (CFU/mL))													
	SCFF13	SCFF15	SCFF18	SCFF20	SCFF104	SCFF109	SCFF125	SCFF127	SCFF134	SCFF180	SCFF193	SCFF195	SCFF220	SCFF240
0	8.74±0.01a	8.87±0.01a	8.71±0.00a	9.12±0.01a	8.56±0.02a	8.73±0.02a	9.24±0.01a	8.69±0.00a	8.68±0.00a	9.07±0.01a	7.63±0.02d	8.15±0.04b	8.11±0.01a	8.21±0.04b
20	8.64±0.01c	8.54±0.02c	8.44±0.01b	8.77±0.01d	8.53±0.02a	8.30±0.00c	8.47±0.00c	8.53±0.02b	8.66±0.04a	8.43±0.03c	7.67±0.02d	7.7±0.01cd	7.60±0.02b	7.66±0.01c
40	8.43±0.01d	8.00±0.00d	8.26±0.01d	8.74±0.01b	8.08±0.01b	8.14±0.01d	8.54±0.00c	8.51±0.05b	8.51±0.01b	8.28±0.02d	8.51±0.01b	7.65±0.01d	6.61±0.03d	7.75±0.01c
60	8.72±0.00b	8.79±0.02b	8.32±0.00c	8.60±0.00c	8.18±0.00b	8.27±0.01c	8.55±0.05b	8.40±0.01c	8.49±0.00b	8.54±0.01b	8.83±0.01a	7.62±0.01d	7.29±0.02c	8.13±0.01b
80	8.82±0.03f	8.87±0.02a	7.72±0.02f	8.71±0.03b	7.91±0.03c	7.81±0.05e	7.66±0.02e	8.21±0.01d	8.09±0.01c	8.12±0.02d	7.27±0.01d	8.94±0.02a	6.25±0.02d	9.06±0.01a
100	8.14±0.02e	8.72±0.02b	8.22±0.01d	8.58±0.02c	7.89±0.01c	8.40±0.01b	8.59±0.01b	8.22±0.03d	8.57±0.01b	8.13±0.01d	8.55±0.01b	8.1±0.01bc	7.27±0.01c	7.76±0.02c
120	8.62±0.02f	8.59±0.03c	8.10±0.03e	8.23±0.01d	7.74±0.02c	7.92±0.02e	7.79±0.01e	8.20±0.02d	7.87±0.01c	8.12±0.02d	8.46±0.01c	8.24±0.01b	5.81±0.02d	8.11±0.02b

Data within each line marked with different letters (a, b, c, d, e, f) indicate significant differences ($P<0.05$).

Table 2 The color characteristics of the bacterial culture solutions, indicated by a* value, after incubation in an MRS medium supplemented with different concentrations of Na₂SeO₃

Na₂SeO₃ (μg/mL)	a* value													
	SCFF13	SCFF15	SCFF18	SCFF20	SCFF104	SCFF109	SCFF125	SCFF127	SCFF134	SCFF180	SCFF193	SCFF195	SCFF220	SCFF240
0	1.39±0.02e	1.44±0.05d	−0.14±0.02f	−0.14±0.04d	−0.01±0.07d	−0.05±0.06e	1.23±0.04e	0.06±0.07c	0.15±0.07d	0.35±0.02e	1.07±0.05d	1.85±0.03e	1.43±0.07d	0.96±0.10e
20	2.04±0.02c	1.95±0.01c	0.34±0.06e	0.58±0.17c	0.06±0.03d	0.49±0.02d	1.44±0.10e	0.22±0.08c	0.73±0.06c	0.90±0.09d	1.38±0.06cd	2.92±0.32bc	3.41±0.05a	1.83±0.04d
40	1.80±0.06d	1.39±0.06d	1.12±0.02d	1.10±0.05c	1.32±0.03b	1.54±0.09b	1.56±0.20c	1.46±0.08a	1.36±0.11b	1.41±0.02c	1.49±0.07bc	3.92±0.03a	1.31±0.04d	2.50±0.12c
60	2.62±0.12a	2.54±0.04a	2.70±0.16a	2.36±0.08b	0.87±0.09c	1.68±0.08a	2.15±0.06d	1.42±0.04ab	1.92±0.04a	1.95±0.05a	1.82±0.10a	3.25±0.04b	2.22±0.01c	3.35±0.19b
80	2.42±0.02ab	2.14±0.05b	1.15±0.10d	2.89±0.11b	0.90±0.10c	1.69±0.04ab	3.41±0.13b	1.21±0.05ab	1.66±0.12ab	1.78±0.09ab	1.81±0.08a	2.14±0.08de	2.32±0.03c	3.01±0.10b
100	2.01±0.01cd	2.24±0.04b	1.82±0.06b	4.26±0.29a	1.75±0.13a	1.81±0.04ab	4.08±0.11a	1.14±0.10b	1.69±0.12a	1.66±0.04bc	1.79±0.15ab	3.83±0.09a	2.34±0.04c	4.21±0.08a
120	2.29±0.01b	1.48±0.08d	1.46±0.10c	4.08±0.09a	1.13±0.01bc	1.25±0.05c	2.87±0.02c	1.47±0.11a	1.81±0.05a	1.94±0.07a	1.96±0.06a	2.51±0.04cd	2.87±0.06b	3.37±0.15b

Additionally, significant differences ($P<0.05$) are denoted by different letters (a, b, c, d, e, f) within each line of data.

Figure 1　The color comparison between (A) the control group (without SeO_3^{2-}) and (B) the treatment group (with SeO_3^{2-}) at the highest a* values for 14 bacterial cultures. SCFF13: *Lactiplantibacillus plantarum* SCFF13; SCFF15: *Lacticaseibacillus paracasei* SCFF15; SCFF18: *Pediococcus pentosaceus* SCFF18; SCFF20: *Lacticaseibacillus paracasei* SCFF20; SCFF104: *Levilactobacillus brevis* SCFF104; SCFF109: *Lactiplantibacillus plantarum* SCFF109; SCFF125: *Pediococcus pentosaceus* SCFF125; SCFF127: *Lentilactobacillus buchneri* SCFF127; SCFF134: *Lactiplantibacillus plantarum* SCFF134; SCFF180: *Lactiplantibacillus plantarum* SCFF180; SCFF193: *Lactiplantibacillus plantarum* SCFF193; SCFF195: *Lactiplantibacillus plantarum* SCFF195; SCFF220: *Limosilactobacillus fermentum* SCFF220; SCFF240: *Lactococcus lactis* SCFF240.

as shown in Figure 2A. As the shaking speed increased, the amount of Se(0) progressively increased up to a rotation of 180 r/min. However, when the shaking speed continued to increase to 240 r/min, the amount of Se(0) tended to be stable and did not increase significantly. Consequently, the optimal shaking speed for the selenate reduction was determined to be 180 r/min (Figure 2B).

The amount of Se(0) was observed to be low when the Se(IV) exposure time was either longer or shorter than 24 h. Hence, the optimum Se(IV) exposure time for the selenate reduction was determined to be 24 h (Figure 2C). The amount of Se(0) increased with the inoculum volume of *L. paracasei* SCFF20 up to an inoculum volume of 3%. However, when the inoculum volume exceeded 3%, the amount of Se(0) started to

decrease. Therefore, the optimum inoculum volume of *L. paracasei* SCFF20 was determined to be 3% (Figure 2D).

The results of varying the Se(IV) concentration in the medium on the growth of *L. paracasei* SCFF20 are presented in Figure 2E. With the increase in the concentration of Na_2SeO_3 in the medium, the amount of Se(0) exhibited an upward trend. Furthermore, at Se(IV) concentrations ranging from 120 to 140 μg/mL, the amount of Se(0) reached its maximum capacity, and there was no significant difference between these two concentrations. Therefore, 120 μg/mL was selected as the optimum Se(IV) concentration for Se-reduction. Finally, *L. paracasei* SCFF20 was subjected to reduction of Na_2SeO_3 into SeNPs under the optimized conditions for the characterization and determination of SeNPs content.
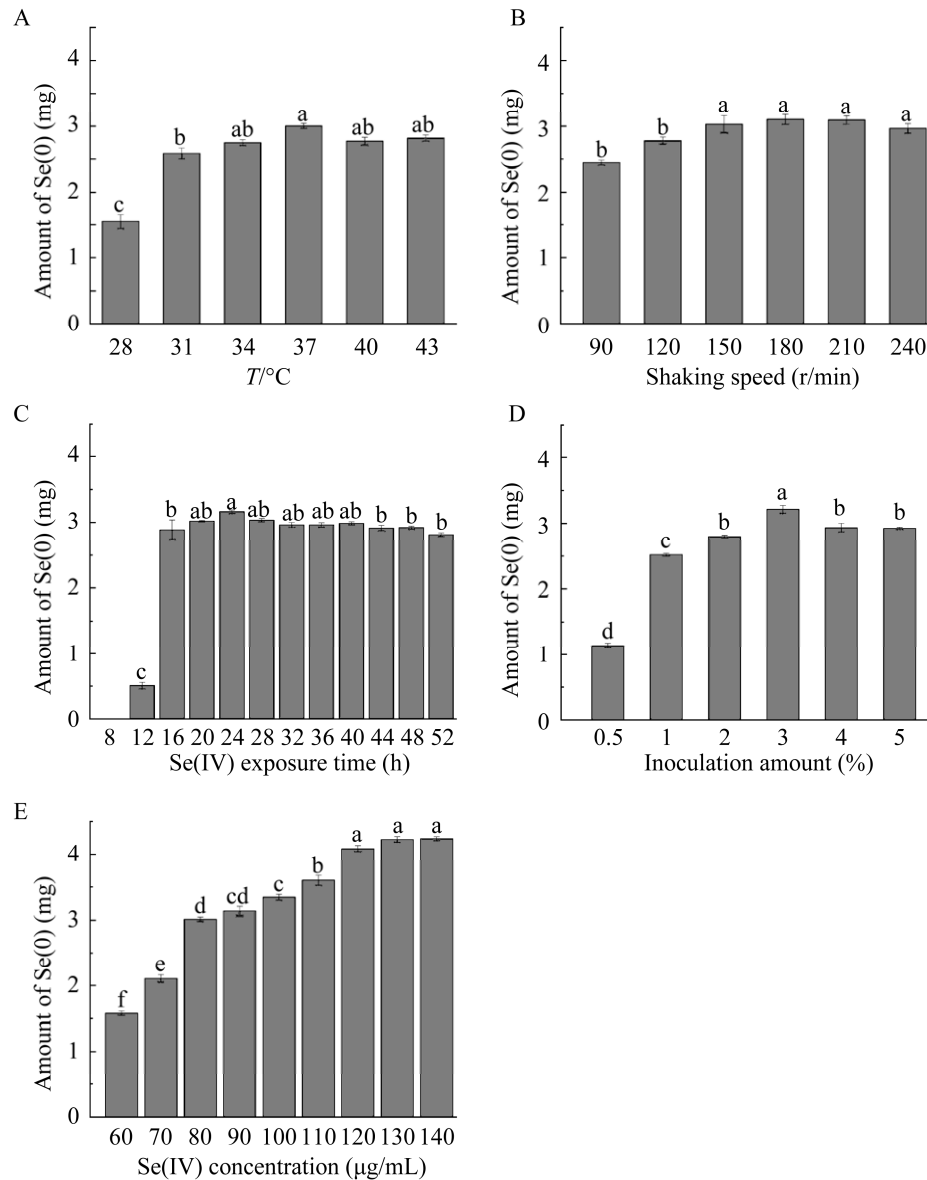
Figure 2   The impact of temperature (A), shaking speed (B), Se(IV) exposure time (C), inoculation amount (D), and Se(IV) concentration (E) on the Se-reduction capability of *Lacticaseibacillus paracasei* SCFF20.

2.3   SEM-EDX analysis of SeNPs

The surface morphologies of SeNPs extracted from *L. paracasei* SCFF20 cultured in an MRS medium with and without Na_2SeO_3 were visualized in Figure 3. The analysis revealed the presence of numerous spherical-shaped nanoparticles distributed around the rod-shaped bacteria (Figure 3B). In contrast, no particles were observed in the control group without the addition of Na_2SeO_3 (Figure 3A), providing evidence the biogenesis of SeNPs from sodium selenite.

Additionally, SEM images showed that isolated SeNPs presented particles (Figure 3C).

To determine the elemental composition of the SeNPs, EDX spectrum analysis was carried out (Figure 3D). When cultured in the presence of Na_2SeO_3, the EDX spectrum exhibited signals corresponding to carbon (C), oxygen (O), and selenium (Se). The atomic percentages of these elements in the biomass of *L. paracasei* SCFF20 were determined to be 46.16% for C, 8.87% for O, and 44.97% for Se.
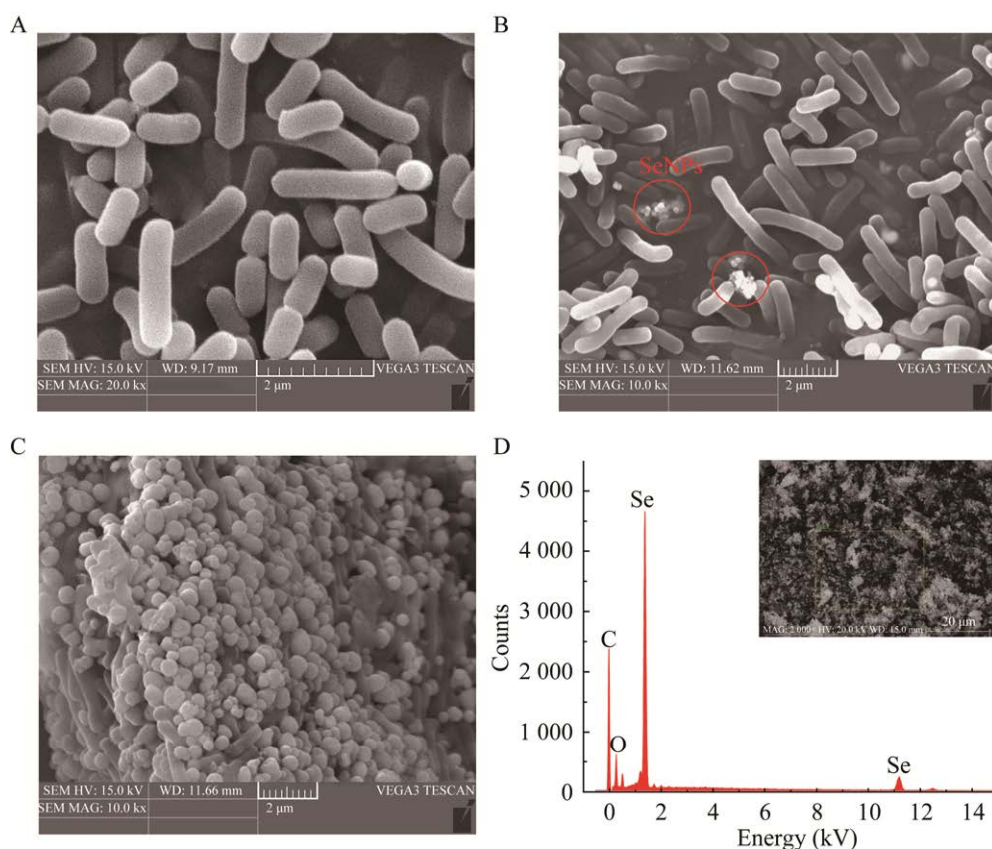
Figure 3 Scanning electron microscopy (SEM) images of extracted SeNPs synthesized by *Lacticaseibacillus paracasei* SCFF20 under two different culture conditions, namely (A) in the absence of SeO_3^{2-} and (B) in the presence of SeO_3^{2-}. The SEM micrographs (C) showcased the purified SeNPs, while the energy-dispersive X-ray (EDX) spectroscopy (EDX) analysis (D) provided the corresponding elemental spectrum of the purified SeNPs. Scanning electron microscopy (SEM) images of extracted SeNPs synthesized (A, B). The SEM micrographs (C) showcased the purified SeNPs, while the energy-dispersive X-ray (EDX) spectroscopy analysis (D) provided the corresponding elemental spectrum of the purified SeNPs. Note: (A) in the absence of SeO_3^{2-} and (B) in the presence of SeO_3^{2-}.

Notably, the strong peaks at 1.35 kV and 11.25 kV were attributed to the characteristic absorption signals from elemental Se. This observation aligns with previous studies[39]. The EDX spectrum confirmed the exclusive presence of elemental Se within the nanoparticles. It is worth mentioning that additional peaks of carbon and oxygen can be attributed to the surface plasmon resonance originating from the protein molecules, which likely participate in capping the nanoparticles produced by bacteria, as discussed by Kora et al.[40] These findings are consistent with earlier investigations conducted on SeNPs synthesized by *Pseudomonas aeruginosa*[40] and *Streptomyces minutiscleroticus*[41].

2.4 DLS analysis

Figure 4 illustrates the utilization of dynamic light scattering (DLS) analysis to determine the average diameter of SeNPs. The DLS measurement revealed that the size of the SeNPs ranged from 295 to 955 nm, with an average hydrodynamic size of 500.62 nm and a polydispersity index (Pdl) of 0.216. It should be noted that a Pdl value smaller than 0.300 is considered necessary for reliable measurement[42]. This finding suggests that the biogenic SeNPs produced by *L. paracasei* SCFF20 are predominantly dispersed and exhibit minimal aggregation. The particle size results obtained in this study are
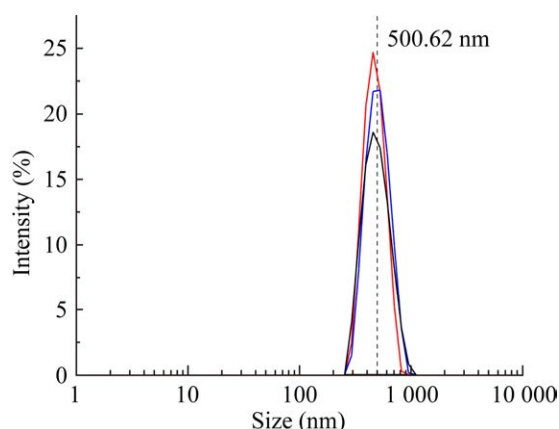
Figure 4　The size distribution of SeNPs synthesized. Three lines of different colors represent three parallel measurements of SeNPs size.

consistent with those reported in the literature for biologically synthesized SeNPs using probiotic *Bacillus subtilis*[18]. However, the size distribution of SeNPs synthesized by some lactic acid bacteria (LAB, such as *Lactobacillus acidophilus*, *Lactobacillus delbrueckii* subsp. *bulgaricus*, and *Lactobacillus reuteri*) provided an average size of 247 nm[43].

2.5　Raman spectroscopy and XRD analysis

To investigate the phase and composition of the synthesized SeNPs, X-ray diffraction (XRD) and Raman spectroscopy were employed for characterization purpose (Figure 5). The crystal structure of the SeNPs was analyzed using XRD (Figure 5A). The XRD results indicated the absence of well-defined Bragg reflections, apart from a broad peak at the 2θ angles of 15°–30°, similar to the control. This observation confirms

the amorphous nature of the synthesized SeNPs[15,40]. The XRD findings were substantiated by the Raman spectroscopy results.

In the Raman spectra of SeNPs (Figure 5B), a single strong band appeared at 250 cm^{-1}, which corresponds to the A1 stretching Se−Se mode and is specifically associated with intrachain stretching of amorphous selenium. Compared to the control group without adding Na_2SeO_3, the increased half-width of this band (b) (approximately 30 cm^{-1}) further supports the presence of amorphous selenium[44]. The absence of other distinguishable lower-frequency bands, except for the peak at 250 cm^{-1}, provides additional evidence for the amorphous structure of the SeNPs derived from biological sources. It is worth noting that other studies have reported peaks at 251 cm^{-1} and 252 cm^{-1} in the Raman spectra of amorphous SeNPs[45]. Furthermore, according to Vineeth Kumar et al.[46], in the Raman spectra of SeNPs obtained from non-biological sources through the chemical reduction of Na_2SeO_3 with cysteine, a strong and narrow characteristic peaks at 236 cm^{-1}, along with a weak shoulder peak at 254 cm^{-1}, are typically observed, in addition to the peak at 250 cm^{-1}.

2.6　FTIR analysis

The cellular functional groups involved in the response to Se(IV) were characterized through Fourier transform infrared spectroscopy (FTIR), and the relevant peaks in the FTIR spectra are depicted in Figure 6. The FTIR spectrum of the synthesized SeNPs exhibited distinct peaks, indicating
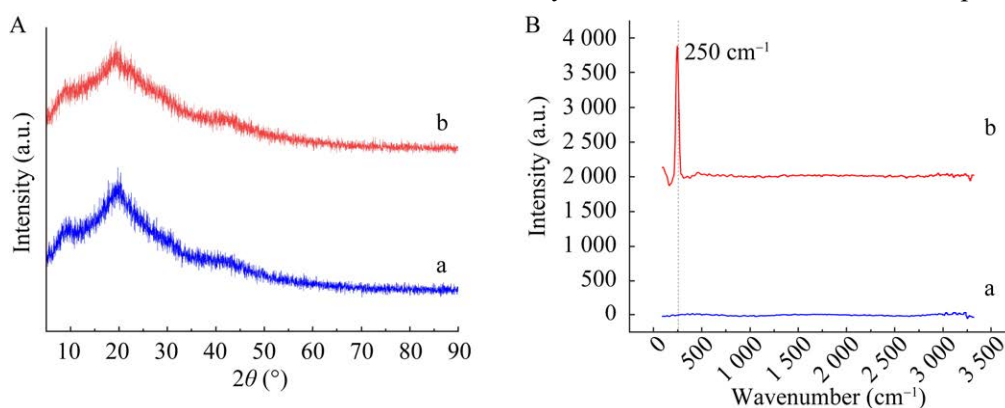

Figure 5　The X-ray diffraction (XRD) patterns (A) and Raman spectra (B) of the SeNPs synthesized by *Lacticaseibacillus paracasei* SCFF20 under two different culture conditions, namely (a) in the absence of SeO_3^{2-} and (b) in the presence of SeO_3^{2-}.
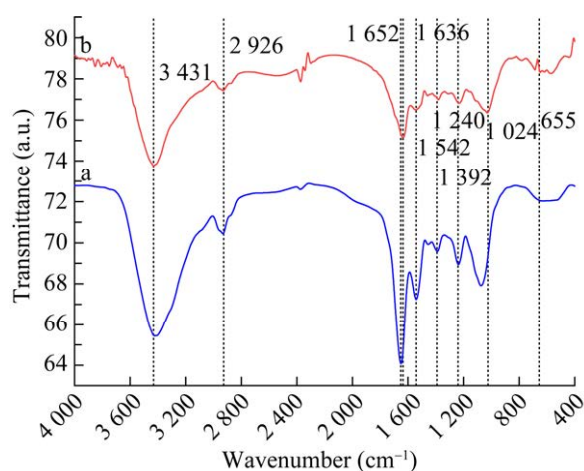
Figure 6　The Fourier transform infrared (FTIR) spectral analysis on the SeNPs synthesized by *Lacticaseibacillus paracasei* SCFF20 under two different culture conditions, namely (a) in the absence of SeO_3^{2-} and (b) in the presence of SeO_3^{2-}.

the presence of various capped biomacromolecules on the surface of nanoparticle. The SeNPs displayed prominent peaks at 3 431 cm^{-1}, which can be attributed to the O–H stretching in molecular water and the N–H stretching in proteins[47]. Notably, compared to that of pure cell culture without adding SeO_3^{2-} (1 652 cm^{-1}), the amide I band (1 636 cm^{-1}) of the proteins capping the SeNPs displayed the lower frequency, suggesting that the secondary structure of the proteins in the bacterial cells represented by dominating α-helix evidently differs from the disordered secondary structure of the proteins capping the surface of SeNPs[48].

Furthermore, the characteristic bands of proteins, including amide II at 1 542 cm^{-1} and amide III at 1 240 cm^{-1}, were evident. These aligns with the previous finding[49], indicating that nanoparticles bond with proteins improved their stabilization and biological activity. The absorption characteristics of the typical vibrational region of polysaccharides (within 1 200–950 cm^{-1}) were also observed[48]. The presence of carboxylate groups in the produced SeNPs indicated by the spectrum band at 1 392 cm^{-1}, corresponding to the symmetric stretching *vs*. (COO−) group. The stretching vibration of the carboxyl group (C=O)

was reflected by the peaks at 1 024 cm^{-1}. The spectrum band at 2 926 cm^{-1} represented the asymmetric stretching vibrations of methylene groups in SeNPs[39,50], while the peak at 655 cm^{-1} could be attributed to the C−X stretching of alkyl halides[30]. Collectively, these data suggest that the SeNPs produced by *L. paracasei* SCFF20 were capped with proteins, exopolysaccharides, and lipids.

2.7　SeNPs content determination

The content of SeNPs synthesized by *L. paracasei* SCFF20 in the presence of SeO_3^{2-} was determined using ICP-OES. The analysis revealed that under optimized conditions, the content of SeNPs reached (6.67±0.07) mg/L, indicating a reduction ability of Na_2SeO_3 into SeNPs of 91.42%, compared to the control samples with a content of <0.05 mg/L. These findings indicate the efficient capability of *L. paracasei* SCCF19 in reducing Na_2SeO_3 into SeNPs.

3　Conclusion

In this study, a Se-resistant strain of *L. paracasei* SCFF20 was selected from a total of 14 potential probiotics, through a series of screening processes including Se-tolerance domestication, and optimization of the fermentation conditions. *L. paracasei* SCFF20 exhibited a noteworthy ability in the biotransformation of toxic soluble selenite into insoluble SeNPs, which possessed an average size of 500.62 nm.

Furthermore, the biogenic SeNPs displayed amorphous morphology, and spherical shape, and were enveloped by proteins, exopolysaccharides, and lipids. As a result, *L. paracasei* SCFF20 holds a great potential as a probiotic strain for SeNP synthesis, thereby serving as a promising vehicle for the delivery of biologically active selenium molecules to the host. The innovative approach of biosynthesizing SeNPs using *L. paracasei* SCFF20 offers a novel strategy for the development of a micro-ecological selenium supplement, exhibiting superior efficacy and enhanced bioavailability. Additionally, the environmentally friendly protocol for scaling up the production of SeNPs using *L. paracasei* SCFF20 can be effectively

employed in commercial applications aimed at enhancing nutritional status.

CRediT authorship contribution statement

ZHAO Zhifeng: Conceptualization, methodology, supervision, writing-review & editing. CAO Yulan: Conceptualization, methodology, formal analysis, investigation, formal analysis, writing-original draft. CHEN Xiaodie: Supervision, validation, writing-review & editing. WANG Zuojun: Supervision, validation, writing-review. XU Teng: Supervision, Writing-editing. XIONG Dake: Supervision, validation. HU Lujun: Conceptualization, methodology, investigation, data curation, formal analysis, supervision, writing-original draft, writing-review & editing, funding acquisition.

Declaration of competing interest

The authors declare that they have no known competing financial interests or personal relationships that could have appeared to influence the work reported in this paper.

Data availability

Data will be made available on request.

Reference

[1] XU CL, QIAO L, GUO Y, MA L, CHENG YY. Preparation, characteristics and antioxidant activity of polysaccharides and proteins-capped selenium nanoparticles synthesized by *Lactobacillus casei* ATCC 393[J]. Carbohydrate Polymers, 2018, 195: 576-585.

[2] GARBISU C, GONZALEZ S, YANG WH, YEE BC, CARLSON DL, YEE A, SMITH NR, OTERO R, BUCHANAN BB, LEIGHTON T. Physiological mechanisms regulating the conversion of selenite to elemental selenium by *Bacillus subtilis*[J]. BioFactors, 1995, 5(1): 29-37.

[3] PALOMO M, GUTIÉRREZ AM, PÉREZ-CONDE MC, CÁMARA C, MADRID Y. Se metallomics during lactic fermentation of Se-enriched yogurt[J]. Food Chemistry, 2014, 164: 371-379.

[4] PESCUMA M, GOMEZ-GOMEZ B, PEREZ-CORONA T, FONT G, MADRID Y, MOZZI F. Food prospects of selenium enriched-*Lactobacillus acidophilus* CRL 636 and *Lactobacillus reuteri* CRL 1101[J]. Journal of Functional Foods, 2017, 35: 466-473.

[5] PEDRERO Z, MADRID Y, CÁMARA C. Selenium species bioaccessibility in enriched radish (*Raphanus sativus*): a potential dietary source of selenium[J]. Journal of Agricultural and Food Chemistry, 2006, 54(6): 2412-2417.

[6] MÖRSCHBÄCHER AP, DULLIUS A, DULLIUS CH, BANDT CR, KUHN D, BRIETZKE DT, JOSÉ MALMANN KUFFEL F, ETGETON HP, ALTMAYER T, GONÇALVES TE, SCHWEIZER YA, ORESTE EQ, RIBEIRO AS, LEHN DN, VOLKEN de SOUZA CF, HOEHNE L. Assessment of selenium bioaccumulation in lactic acid bacteria[J]. Journal of Dairy Science, 2018, 101(12): 10626-10635.

[7] RODRÍGUEZ-HERNÁNDEZ Á, ZUMBADO M, HENRÍQUEZ-HERNÁNDEZ LA, BOADA LD, LUZARDO OP. Dietary intake of essential, toxic, and potentially toxic elements from mussels (*Mytilus* spp.) in the Spanish population: a nutritional assessment[J]. Nutrients, 2019, 11(4): 864.

[8] ZHANG BW, ZHOU K, ZHANG JL, CHEN Q, LIU GR, SHANG N, QIN W, LI PL, LIN FX. Accumulation and species distribution of selenium in Se-enriched bacterial cells of the *Bifidobacterium animalis* 01[J]. Food Chemistry, 2009, 115(2): 727-734.

[9] PRASAD KS, PATEL H, PATEL T, PATEL K, SELVARAJ K. Biosynthesis of Se nanoparticles and its effect on UV-induced DNA damage[J]. Colloids and Surfaces B: Biointerfaces, 2013, 103: 261-266.

[10] PORTO BAA, MANGIAPANE E, PESSIONE A, NEVES MJ, PESSIONE E, MARTINS FS. Evaluation of sodium selenite effects on the potential probiotic *Saccharomyces cerevisiae* UFMG A-905: a physiological and proteomic analysis[J]. Journal of Functional Foods, 2015, 17: 828-836.

[11] PIENIZ S, ANDREAZZA R, MANN MB, CAMARGO F, BRANDELLI A. Bioaccumulation and distribution of selenium in *Enterococcus durans*[J]. Journal of Trace Elements in Medicine and Biology, 2017, 40: 37-45.

[12] VOGEL M, FISCHER S, MAFFERT A, HÜBNER R, SCHEINOST AC, FRANZEN C, STEUDTNER R. Biotransformation and detoxification of selenite by microbial biogenesis of selenium-sulfur nanoparticles[J]. Journal of Hazardous Materials, 2018, 344: 749-757.

[13] DONG Y, ZHANG HT, HAWTHORN L, GANTHER HE, IP C. Delineation of the molecular basis for selenium-induced growth arrest in human prostate cancer cells by oligonucleotide array[J]. Cancer Research, 2003, 63(1): 52-59.

[14] SANTELLI CM, SABUDA MC, ROSENFELD CE. Time-resolved examination of fungal selenium redox transformations[J]. ACS Earth and Space Chemistry, 2023, 7(5): 960-971.

[15] HUSEN A, SIDDIQI KS. Plants and microbes assisted selenium nanoparticles: characterization and application[J]. Journal of Nanobiotechnology, 2014, 12: 28.

[16] ZHANG SY, ZHANG J, WANG HY, CHEN HY. Synthesis of selenium nanoparticles in the presence of polysaccharides[J]. Materials Letters, 2004, 58(21): 2590-2594.

[17] CUI YH, LI LL, ZHOU NQ, LIU JH, HUANG Q, WANG HJ, TIAN J, YU HQ. *In vivo* synthesis of nano-selenium by *Tetrahymena thermophila* SB210[J]. Enzyme and Microbial Technology, 2016, 95: 185-191.

[18] ULLAH A, YIN X, WANG FH, XU B, MIRANI ZA, XU BC, CHAN MWH, ALI A, USMAN M, ALI N, NAVEED M. Biosynthesis of selenium nanoparticles (*via Bacillus subtilis* BSN313), and their isolation, characterization, and bioactivities[J]. Molecules, 2021, 26(18): 5559.

[19] LI ZJ, WANG QQ, DAI FJ, LI HF. Reduction of selenite to selenium nanospheres by Se(IV)-resistant *Lactobacillus paralimentarius* JZ07[J]. Food Chemistry, 2022, 393: 133385.

[20] POPHALY SD, SINGH P, KUMAR H, TOMAR SK, SINGH R. Selenium enrichment of lactic acid bacteria and bifidobacteria: a functional food perspective[J]. Trends in Food Science & Technology, 2014, 39(2): 135-145.

[21] YAZDI MH, MAHDAVI M, SETAYESH N, ESFANDYAR M, SHAHVERDI AR. Selenium nanoparticle-enriched *Lactobacillus brevis* causes more efficient immune responses *in vivo* and reduces the liver metastasis in metastatic form of mouse breast cancer[J]. DARU Journal of Pharmaceutical Sciences, 2013, 21(1): 33.

[22] ANDREONI V, LUISCHI MM, CAVALCA L, ERBA D, CIAPPELLANO S. Selenite tolerance and accumulation in the *Lactobacillus* species[J]. Annals of Microbiology, 2000, 50: 77-88.

[23] ENDO A, MAENO S, TANIZAWA Y, KNEIFEL W, ARITA M, DICKS L, SALMINEN S. Fructophilic lactic acid bacteria, a unique group of fructose-fermenting microbes[J]. Applied and Environmental Microbiology, 2018, 84(19): e01290-18.

[24] SUN YH, GAN Y, ZHANG L, SHI YH, YUE TL, YUAN YH. Isolation and identification of *Monascus* and evaluation of its selenium accumulation[J]. LWT, 2022, 154: 112887.

[25] SUHAJDA Á, HEGÓCZKI J, JANZSÓ B, PAIS I, VERECZKEY G. Preparation of selenium yeasts I. preparation of selenium-enriched *Saccharomyces cerevisiae*[J]. Journal of Trace Elements in Medicine and Biology, 2000, 14(1): 43-47.

[26] SAINI K, TOMAR SK, SANGWAN V, BHUSHAN B. Evaluation of lactobacilli from human sources for uptake and accumulation of selenium[J]. Biological Trace Element Research, 2014, 160(3): 433-436.

[27] CHEN XD, LIN M, HU LJ, XU T, XIONG DK, LI L, ZHAO ZF. Research on the effect of simultaneous and sequential fermentation with *Saccharomyces cerevisiae* and *Lactobacillus plantarum* on antioxidant activity and flavor of apple cider[J]. Fermentation, 2023, 9(2): 102.

[28] BISWAS KC, BARTON LL, TSUI WL, SHUMAN K, GILLESPIE J, EZE CS. A novel method for the measurement of elemental selenium produced by bacterial reduction of selenite[J]. Journal of Microbiological Methods, 2011, 86(2): 140-144.

[29] SONKUSRE P. Improved extraction of intracellular biogenic selenium nanoparticles and their specificity for cancer chemoprevention[J]. Journal of Nanomedicine & Nanotechnology, 2014, 5(2): 1000194

[30] AL-HAGAR OEA, ABOL-FOTOUH D, ABDELKHALEK ES, ABO ELSOUD MM, SIDKEY NM. *Bacillus niabensis* OAB2: outstanding bio-factory of selenium nanoparticles[J]. Materials Chemistry and Physics, 2021, 273: 125147.

[31] MARTÍNEZ FG, MORENO-MARTIN G, PESCUMA M, MADRID-ALBARRÁN Y, MOZZI F. Biotransformation of selenium by lactic acid bacteria: formation of seleno-nanoparticles and seleno-amino acids[J]. Frontiers in Bioengineering and Biotechnology, 2020, 8: 506.

[32] ZHANG GC, YAO XY, WANG CL, WANG DH, WEI GY. Transcriptome analysis reveals the mechanism underlying improved glutathione biosynthesis and secretion in *Candida utilis* during selenium enrichment[J]. Journal of Biotechnology, 2019, 304: 89-96.

[33] LUO Y, ZHAO ZJ, CHEN HJ, PAN XL, LI RS, WU DW, HU XC, ZHANG LL, WU HW, LI XH. Dynamic

analysis of physicochemical properties and polysaccharide composition during the pile-fermentation of post-fermented tea[J]. Foods, 2022, 11(21): 3376.

[34] HU LT, ELAM E, NI ZJ, SHEN Y, XIA B, THAKUR K, JIANG L, ZHANG JG, WEI ZJ. The structure and flavor of low sodium seasoning salts in combination with different sesame seed meal protein hydrolysate derived Maillard reaction products[J]. Food Chemistry: X, 2021, 12: 100148.

[35] ELMAATY TA, RAOUF S, SAYED-AHMED K, PLUTINO MR. Multifunctional dyeing of wool fabrics using selenium nanoparticles[J]. Polymers, 2022, 14(1): 191.

[36] LORTIE L, GOULD WD, RAJAN S, McCREADY RG, CHENG KJ. Reduction of selenate and selenite to elemental selenium by a *Pseudomonas stutzeri* isolate[J]. Applied and Environmental Microbiology, 1992, 58(12): 4042-4044.

[37] MISHRA RR, PRAJAPATI S, DAS J, DANGAR TK, DAS N, THATOI H. Reduction of selenite to red elemental selenium by moderately halotolerant *Bacillus megaterium* strains isolated from Bhitarkanika mangrove soil and characterization of reduced product[J]. Chemosphere, 2011, 84(9): 1231-1237.

[38] BAJAJ M, SCHMIDT S, WINTER J. Formation of Se(0) nanoparticles by *Duganella* sp. and *Agrobacterium* sp. isolated from Se-laden soil of north-east Punjab, India[J]. Microbial Cell Factories, 2012, 11: 64.

[39] YILMAZ MT, İSPIRLI H, TAYLAN O, DERTLI E. A green nano-biosynthesis of selenium nanoparticles with *Tarragon* extract: structural, thermal, and antimicrobial characterization[J]. LWT, 2021, 141: 110969.

[40] KORA AJ, RASTOGI L. Biomimetic synthesis of selenium nanoparticles by *Pseudomonas aeruginosa* ATCC 27853: an approach for conversion of selenite[J]. Journal of Environmental Management, 2016, 181: 231-236.

[41] RAMYA S, SHANMUGASUNDARAM T, BALAGURUNATHAN R. Biomedical potential of actinobacterially synthesized selenium nanoparticles with special reference to anti-biofilm, anti-oxidant, wound healing, cytotoxic and anti-viral activities[J]. Journal of Trace Elements in Medicine and Biology, 2015, 32: 30-39.

[42] LIN ZC, HWANG TL, HUANG TH, TAHARA K, TROUSIL J, FANG JY. Monovalent antibody-conjugated lipid-polymer nanohybrids for active targeting to desmoglein 3 of keratinocytes to attenuate psoriasiform inflammation[J]. Theranostics, 2021, 11(10): 4567-4584.

[43] MORENO-MARTIN G, PESCUMA M, PÉREZ-CORONA T, MOZZI F, MADRID Y. Determination of size and mass-and number-based concentration of biogenic SeNPs synthesized by lactic acid bacteria by using a multimethod approach[J]. Analytica Chimica Acta, 2017, 992: 34-41.

[44] TUGAROVA AV, MAMCHENKOVA PV, DYATLOVA YA, KAMNEV AA. FTIR and Raman spectroscopic studies of selenium nanoparticles synthesised by the bacterium *Azospirillum thiophilum*[J]. Spectrochimica Acta Part A: Molecular and Biomolecular Spectroscopy, 2018, 192: 458-463.

[45] PINTO AH, LEITE ER, LONGO E, de CAMARGO ER. Crystallization at room temperature from amorphous to trigonal selenium as a byproduct of the synthesis of water dispersible zinc selenide[J]. Materials Letters, 2012, 87: 62-65.

[46] VINEETH KUMAR CM, KARTHICK V, INBAKANDAN D, KUMAR VG, RENE ER, DHAS TS, RAVI M, SOWMIYA P, ANJALI DAS CG. Effect of selenium nanoparticles induced toxicity on the marine diatom *Chaetoceros gracilis*[J]. Process Safety and Environmental Protection, 2022, 163: 200-209.

[47] SHAKIBAIE M, FOROOTANFAR H, MOLLAZADEH-MOGHADDAM K, BAGHERZADEH Z, NAFISSI-VARCHEH N, SHAHVERDI AR, FARAMARZI MA. Green synthesis of gold nanoparticles by the marine microalga *Tetraselmis suecica*[J]. Biotechnology and Applied Biochemistry, 2010, 57(2): 71-75.

[48] KAMNEV AA, MAMCHENKOVA PV, DYATLOVA YA, TUGAROVA AV. FTIR spectroscopic studies of selenite reduction by cells of the rhizobacterium *Azospirillum brasilense* Sp7 and the formation of selenium nanoparticles[J]. Journal of Molecular Structure, 2017, 1140: 106-112.

[49] GOLE A, DASH C, RAMAKRISHNAN V, SAINKAR SR, MANDALE AB, RAO ML, SASTRY M. Pepsin-gold colloid conjugates: preparation, characterization, and enzymatic activity[J]. Langmuir, 2001, 17(5): 1674-1679.

[50] KORA AJ, RASTOGI L. Bacteriogenic synthesis of selenium nanoparticles by *Escherichia coli* ATCC 35218 and its structural characterisation[J]. IET Nanobiotechnology, 2017, 11(2): 179-184.